PHYSICAL REVIEW B, VOLUME 65, 041402(R)

Electronic interwall interactions and charge redistribution in multiwall nanotubes

Yoshiyuki Miyamoto,[1] Susumu Saito,[2] and David Tománek[3]
[1]*Fundamental Research Laboratories, NEC Corporation, 34 Miyukigaoka, Tsukuba, 305-8501, Japan*
[2]*Department of Physics, Tokyo Institute of Technology, 2-12-1 Oh-okayama, Meguro-ku, Tokyo 152-8551, Japan*
[3]*Department of Physics and Astronomy, Michigan State University, East Lansing, Michigan 48824-1116*
(Received 9 October 2001; published 28 December 2001)

Using density functional theory, we calculate the charge redistribution incurred upon forming multiwall carbon nanotubes, or by sandwiching initially isolated single-wall nanotubes between graphene layers. In these systems, we observe a significant charge transfer between the π electron system of the tube walls and a newly formed interlayer state. We discuss the direction of charge flow in terms of the interlayer hybridization and work function differences in the composite systems.

DOI: 10.1103/PhysRevB.65.041402 PACS number(s): 61.48.+c, 71.20.Tx, 73.61.Wp, 81.05.Tp

Carbon nanotubes[1] have attracted much attention from the viewpoints of science and technological applications because of their unique electronic and mechanical properties. Prior to experimental confirmation, it was predicted that a single-wall nanotube (SWNT) can be either semiconducting or metallic, depending on its helical pitch and diameter.[2,3] Whereas the conductance behavior of SWNTs can be basically understood based on the electronic structure of a graphene monolayer, there is no such simple relationship to planar graphite for the band structure and density of states of narrow SWNTs. There, the large curvature of the walls causes a hybridization between the σ^* and π^* electron systems which are decoupled in graphite. As a consequence, all SWNTs with a diameter below 7 Å have been predicted to be metallic, independent on their helical pitch.[4]

Further modifications in the electronic structure are introduced due to interwall interaction in multiwall nanotubes (MWNTs). Interest in these systems is rising due to recent synthesis of double-wall nanotubes (DWNTs) by fusion of fullerenes encapsulated in SWNTs.[5,6] Due to low density of states at the Fermi level and close proximity of van Hove singularities, even a minute charge redistribution in nanotubes may significantly modify their conducting and superconducting behavior.[7,8] Drastic effects due to charge transfer are expected in nanotube-based electronic devices.[7] In double-wall nanotubes, theoretical studies have addressed the effect of interwall interactions on the equilibrium geometry[9] and electronic structure.[10] So far, there have been no self-consistent calculations that would focus on the electrostatic potential and charge distribution in nanotubes with multiple walls.

Here we show that the presence of an interwall interaction in DWNTs modifies the electronic states close to the Fermi level, thus revealing the atomic arrangement within both walls to scanning tunneling microscopy (STM)[11] and resonant Raman spectroscopy.[12] Our self-consistent calculations also indicate that, depending on the diameter of the individual tubes, there is a charge transfer that shifts the energy bands by up to 0.3 eV, a significant value in device physics. We find the charge transfer to occur not only from one tube to another, but also to a newly formed interwall state. This state, reminiscent of the interlayer state found in graphite,[13] may affect the conductivity of DWNTs.[14]

Due to the local curvature and rehybridization between the σ^* and π^* states, we suspect the work function of nanotubes to be higher than that of graphite. This appears to be confirmed by the direction of charge flow in a system consisting of nanotubes sandwiched between graphene sheets. Unfortunately, the potential in DWNT systems, consisting of pairs of (n,n) ''armchair'' nanotubes, is different from that of the isolated SWNT components. The direction of charge flow may then not be correlated with SWNT work function differences. The importance of the self-consistent potential is emphasized by the lack of correlation between the work function and tube diameter, when judged by charge transfer only.

In this work, we have performed first-principles calculations using density functional theory within the local density approximation (LDA). For the LDA exchange-correlation potential, we used the Perdew-Zunger functional[15] fitted to the Ceperley-Alder results.[16] Soft nonlocal pseudopotentials[17] in the separable form[18] were used to express interactions between valence electrons and ions. A plane wave basis set with a kinetic cutoff energy of 40 Ry was used to expand the Bloch valence wave functions. In the three-dimensional periodic lattice used in our calculation, we used hexagonal unit cells with the *c* axis parallel to the tube axis. The unit cell size was chosen to keep the distance between the walls of adjacent tubes at 7 Å, to prevent wave function overlap between neighboring cells. To perform the momentum space integration for DWNTs, we sampled the first quasi-1D Brillouin zone by 18*k* points. In the following, we focus mainly on the (5,5)@(10,10) double-wall nanotube, consisting of a (5,5) inside the (10,10) nanotube. We also find this system convenient for the sake of simple comparison with previous calculations.[9,10] We also investigated charge redistribution profiles in other systems, namely (4,4)@(9,9), (4,4)@(10,10), (4,4)@(11,11), (5,5)@(11,11), (6,6)@(11,11), and (6,6)@(12,12) double-wall nanotubes.

When computing the electronic structure of (5,5)@(10,10) nanotubes, we considered two different geometries, one of them symmetric and the other one asymmet-

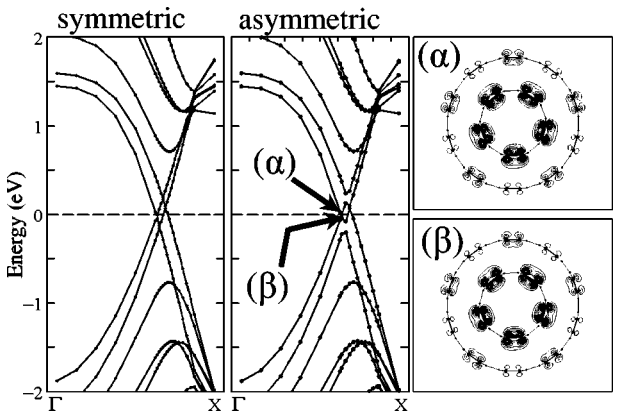

FIG. 1. One-dimensional electronic band structure of the (5,5)@(10,10) double-wall nanotube in the symmetric (left) and asymmetric (middle) configuration. The position of $E_F = 0$ eV is shown by the dashed line. The energy position of pseudogap states α and β, lying 0.03 eV above and below E_F of the asymmetric (5,5)@(10,10) nanotube, is indicated by arrows in the middle panel. The two rightmost panels are contour maps of the charge density associated with these states. The contour plots are shown in a plane containing the atoms, normal to the tube axis. The minimum contour values shown are set to be common.

ric. In both cases the tubes are coaxial. In the symmetric geometry the two nanotubes maintain the common fivefold symmetry. In the asymmetric geometry, which was also considered in Ref. 10, the fivefold symmetry is broken by first rotating the (5,5) nanotube by 3° from the symmetric orientation and then shifting it axially by half a lattice constant. Figure 1 shows the computed band structures of the symmetric and asymmetric (5,5)@(10,10) nanotubes, which resemble those obtained by the tight-binding (TB) method.[10] In the symmetric (5,5)@(10,10) system, four bands cross near the Fermi level. In the asymmetric case, band crossing is not allowed, causing the formation of four pseudogaps in the density of states. Since TB and LDA give similar band structures, the subtle differences in the charge distribution and character of wave functions close to E_F have been missed for a long time. While the inter-layer hybridization opens up pseudogaps in the electronic structure, it also modifies the character of the corresponding wavefunction near E_F, as shown in the rightmost panels of Fig. 1, and hence is likely to affect the conductivity of multiwall nanotubes.[14]

The eigenstate characteristics near E_F of the asymmetric (5,5)@(10,10) nanotubes are displayed in the rightmost panels of Fig. 1 as contour maps of the corresponding charge densities. The state labeled α is located 0.03 eV above E_F, whereas the β state lies 0.03 eV below E_F. These eigenstates are close to the pseudogap region and are predominatly formed by the π orbitals of the inner (5,5) nanotube. Meanwhile, tails of these wave functions extend out to the region occupied by the outer (10,10) nanotube, where they reflect the atomic arrangement of the inner tube. We therefore expect that STM and STS spectra for very small bias voltages, which sample a very narrow energy region around E_F, can provide information about the atomic structure and relative orientation in multiwall nanotubes.[11] This rather subtle effect, confined mainly to the pseudogap region very close to E_F, has been apparently overlooked in previous simulations of STM images of multiwalled nanotubes that were performed for larger bias voltages.[19,20]

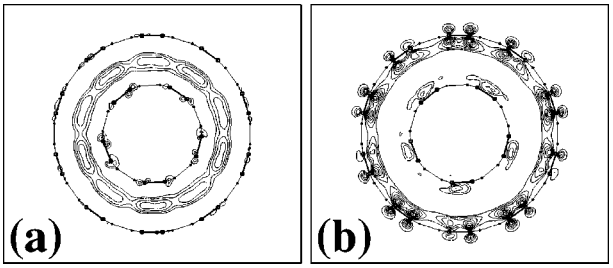

FIG. 2. Contour maps of the accumulated (a) and depleted (b) charge densities within the asymmetric (5,5)@(10,10) nanotube. The contour plots are shown in a plane containing the atoms, normal to the tube axis. The minimum contour values shown are set to be common.

Next we discuss the self-consistent charge redistribution in the (5,5)@(10,10) DWNT. Figure 2(a) displays the accumulated and 2(b) the depleted charge in the asymmetric (5,5)@(10,10) nanotube with respect to the superposition of isolated (5,5) and (10,10) nanotubes. We find it intriguing that the charge transfer does not mainly occur from one tube to another, but rather from the outer (10,10) tube to the intertube region. We find this behavior not to depend on the tube orientation, and to occur for the symmetric (5,5)@(10,10) arrangement as well. We found the amount of charge transfer of 0.09 electrons per period, corresponding to sixty carbon atoms within a 2.46 Å long axial tube segment, to be considerable. The (10,10) nanotube therefore can be viewed as being hole doped by the inner (5,5) nanotube. A very similar charge transfer is also seen in a hypothetical situation, in which arrays of (10,10) nanotubes are sandwiched in-between graphene sheets, as shown in Fig. 3(a).

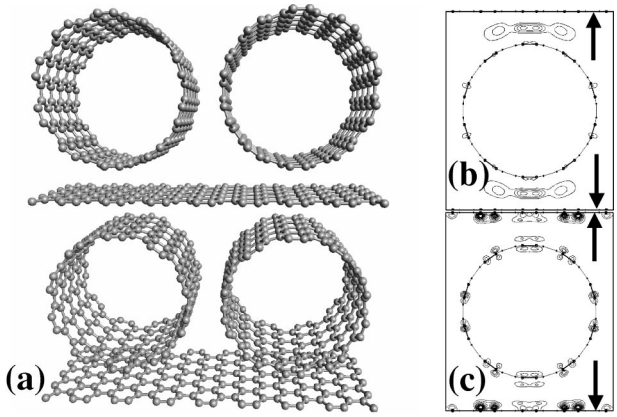

FIG. 3. (a) Perspective view of the atomic arrangement for arrays of (10,10) nanotubes sandwiched between graphene layers. The interwall distance is 3.47 Å between the tubes and 3.34 Å between the tubes and graphene layers. Contour maps of the accumulated (b) and depleted (c) charge densities of the system. The position of the graphene layers is indicated by arrows. The contour plots are shown in a plane containing the atoms, normal to the tube axes. The minimum contour values shown are set to be common.

The character of the state which accommodates the extra charge is very similar to the interlayer state found in graphite.[13] The charge redistribution within this system, shown in Figs. 3(b) and 3(c), is determined by subtracting superposed charge densities of neutral, isolated (10,10) nanotubes and graphene monolayers from the total charge density of the bulk system. As shown in Figs. 3(b) and 3(c), the depleted charge stems from the π electron system of the graphene layers. This result is consistent with the intuitive interpretation that the work function of nanotubes is higher than that of graphite, as confirmed by recent photoemission data.[21] Recently, a similar charge redistribution profile has also been discovered in ''peapods,'' consisting of fullerene chains encapsulated in nanotubes.[22]

Similar charge accumulations in the interwall region were also found in (4,4)@(9,9),(4,4)@(10,10),(4,4)@(11,11), and (6,6)@(11,11) double-wall nanotubes. Among these, the (6,6)@(11,11) DWNT shows a π-electrons depletion of the outer (11,11) nanotube, same as the (5,5)@(10,10) nanotube. On the other hand, in other (4,4)@(n,n) pairs, with n ranging from 9 to 11, the charge depletion occurs in the *inner* (4,4) nanotube. As for the (5,5)@(11,11) and (6,6)@(12,12) nanotubes, the direction of the charge transfer is unclear. Thus we conclude that the direction of charge flow does not simply follow an ordering scheme based on tube diameters, not even for the same helical pitch.

In general, the direction of charge transfer between two weakly interacting systems is determined by the difference of their work functions. An intriguing question is, whether the intertube interaction in multiwall tubes can be considered weak enough to allow the extrapolation of work functions for isolated single-wall tubes.

For solid surfaces, the asymptotic form of the self-consistent potential in the direction normal to the surface was used to determine the work function in a periodic array of slabs.[23] As we show in Fig. 4, the self-consistent potential V_{tot} of the dilute periodic lattice of (5,5)@(10,10) nanotubes does not converge sufficiently fast the intertube region to allow a similar work function extrapolation. This slow convergence is chiefly due to the asymptotic behavior of the Hartree and local-ionic potentials which diverge logarithmically with increasing distance from charged cylindrical objects.[24] Due to the even smaller interwall than intertube distance in DWNTs, the changes in the crystal potential due to the presence of the other tube and the interwall interaction are likely to significantly modify the potential of the individual tubes, making extrapolations of their work function in this geometry even more difficult. We believe that the calculation of accurate work function values for nanotubes of a given diameter and helical pitch is nontrivial, since it requires considering a very large vacuum region away from the tube. We should also note that, in reality, a finite length of nanotubes must affect their work function.

Since the charge flow in a multiwall system is not simply correlated with the work function difference of the individual tubes, we seek in the following to explain its origin in terms of the interwall hybridization. These considerations have to take into account not only the curvature-induced changes in the π electron system of the tubes, but also their interaction

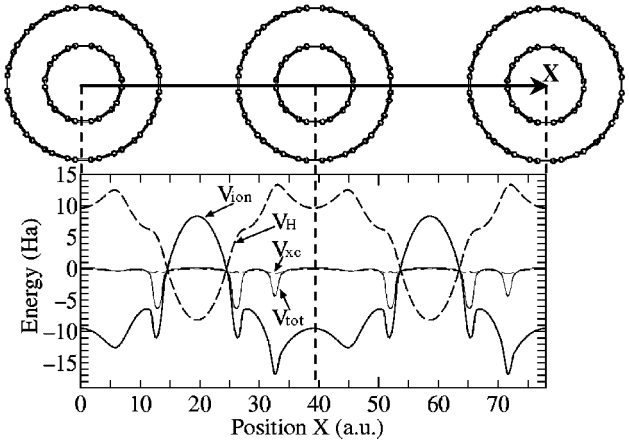

FIG. 4. Profiles of the self-consistent potentials along a line connecting the nearest-neighbor (5,5)@(10,10) double-wall nanotubes in the periodic lattice. V_{tot} stands for the total, V_H for the Hartree, V_{ion} for the ionic, and V_{xc} for the exchange-correlation potential in the lower panel. The contribution of the nonlocal part of the pseudopotentials is not shown. The corresponding atomic positions within the symmetric (5,5)@(10,10) nanotube and the line used to display the potential profiles is given in the upper panel.

with the newly formed interwall state. Our calculations indicate that in planar hexagonal graphite, there is no charge flow into the interlayer region.[25] We conclude that the involvement of the interwall state in the charge redistribution is closely related to the curvature of the tube walls.

As shown in previous calculations,[4] the tube wall curvature causes a σ^*-π^* hybridization which is suppressed by symmetry in planar graphite monolayers. We expect that the modified $\sigma(*)$ and $\pi(*)$ system of electrons will interact with the interlayer state. The degree of rehybridization within the MWNT system, as compared to graphite, depends not only on the curvature of the individual tubes, but even more importantly on the interwall distance and the atomic registry between adjacent walls. Judging from very similar charge redistributions found for the symmetric and asymmetric (5,5)@(10,10) DWNTs, the chirality and diameter of the individual tubes matter more than relative tube orientations. It is difficult to pinpoint the dominant eigenstates responsible for the charge transfer into the interwall region, since the charge redistribution has contributions from many eigenstates, some of them far below E_F. Also, there appears to be a significant hybridization between these deep states and the interlayer state.[22]

The possibility of hole doping of composite systems containing nanotubes and fullerenes without halogen or other impurity atoms, as predicted for the (10,10) nanotube within the (5,5)@(10,10) double-wall system, opens new possibilities for engineered electronic devices. Recently, hole doping was shown to significantly increase the superconducting transition temperature T_C of supported fullerene layers.[26] We expect that hole doping will modify the conductivity of nanotubes, and may even lead to higher T_C values for nanotube-based superconductors.

Finally, we briefly address the exfoliation energy in MWNTs. Due to the curvature-induced reactivity increase,

we expect that the energy to separate nested nanotubes should exceed the exfoliation energy of graphite (0.054 eV/atom experimental,[27] 0.025 eV/atom theoretical.[28]) Our value of 0.07 eV per unit cell containing sixty atoms in total lies significantly lower. We suspect that the present k point sampling, even though finer than in previous work,[9] is still not sufficient enough to probe the density of states in the vicinity of the Fermi level in (5,5)@(10,10) nanotubes with sufficient accuracy. We believe that a precise determination of the exfoliation energy of nanotubes will involve a very dense k point mesh probing the eigenstates near E_F.

In summary, we calculated the self-consistent charge density and potential profiles for double-wall nanotubes, considering constituent tubes of various chiralities, and for single-wall nanotubes sandwiched between graphene layers. We found that the atomic structure of the inner tube modifies the charge density associated with states near E_F even outside the outer tube, so that it can be probed by STM. A significant amount of charge, originating mainly from the π electron system of the tubes and graphite layers, is transferred mainly into a new interwall state, related to the interlayer state of graphite. The associated hole doping, occurring in individual tubes, will affect their conducting and possibly superconducting behavior. Our results indicate that the work function of nanotubes is larger than that of graphite, and that work function differences between single-wall tubes cannot be deduced easily from the charge transfer in double-wall systems.

All calculations were performed on the SX4 supercomputer system at the NEC Tsukuba Laboratories. This work was performed under the management of Frontier Carbon Technology supported by NEDO. This work was also supported by Grant-in-Aid for Scientific Research, Priority Area (#402) by Ministry of Education of Japan, JSPS RFTF96P00203 and Nissan Science Foundation (S.S.); ONR and DARPA under Grant No. N00014-99-1-0252 (D.T.).

[1] S. Iijima, Nature (London) **354**, 56 (1991).
[2] N. Hamada, S. Sawada, and A. Oshiyama, Phys. Rev. Lett. **68**, 1579 (1992).
[3] R. Saito, M. Fujita, G. Dresselhaus, and M.S. Dresselhaus, Appl. Phys. Lett. **60**, 2204 (1992).
[4] X. Blase, L.X. Benedict, E.L. Shirley,and S.G. Louie, Phys. Rev. Lett. **72**, 1878 (1994).
[5] B.W. Smith and D.E. Luzzi, Chem. Phys. Lett. **321**, 169 (2000).
[6] S. Bandow, M. Takizawa, K. Hirahara, M. Yudasaka, and S. Iijima, Chem. Phys. Lett. **337**, 48 (2001).
[7] François Léonard and J. Tersoff, Phys. Rev. Lett. **83**, 5174 (1999).
[8] M. Kociak, A.Yu. Kasumov, S. Guéron, B. Reulet, I.I. Khodos, Yu.B. Gorbatov, V.T. Volkov, L. Vaccarini, and H. Bouchiat, Phys. Rev. Lett. **86**, 2416 (2001).
[9] J.-C. Charlier and J.-P. Michenaud, Phys. Rev. Lett. **70**, 1858 (1993).
[10] Y.K. Kwon and D. Tománek, Phys. Rev. B **58**, R16 001 (1998).
[11] A. Hassanien, M. Tokumoto, and D. Tománek, Appl. Phys. Lett. (to be published).
[12] A. Jorio, R. Saito, J.H. Hafner, C.M. Lieber, M. Hunter, T. McClure, G. Dresselhaus, and M.S. Dresselhaus, Phys. Rev. Lett. **86**, 1118 (2001).
[13] N.A.W. Holzwarth, S.G. Louie, and S. Rabii, Phys. Rev. B **26**, 5382 (1982), and references therein.
[14] Stefano Sanvito, Young-Kyun Kwon, David Tománek, and Colin J. Lambert, Phys. Rev. Lett. **84**, 1974 (2000).
[15] J.P. Perdew and A. Zunger, Phys. Rev. B **23**, 5048 (1981).
[16] D.M. Ceperley and B.J. Alder, Phys. Rev. Lett. **45**, 566 (1980).
[17] N. Troullier and J.L. Martins, Phys. Rev. B **43**, 1993 (1991).
[18] L. Kleinmann and D.M. Bylander, Phys. Rev. Lett. **48**, 1425 (1982).
[19] A. Rubio, Appl. Phys. A: Mater. Sci. Process. **68**, 275 (1999).
[20] Ph. Lambin, V. Meunier, and A. Rubio, Phys. Rev. B **62**, 5129 (2000).
[21] S. Suzuki, C. Bower, Y. Watanabe, and O. Zhou, Appl. Phys. Lett. **76**, 4007 (2000).
[22] S. Okada, S. Saito, and A. Oshiyama, Phys. Rev. Lett. **86**, 3835 (2001).
[23] See, for example, J.R. Chelikowsky, Phys. Rev. B **16**, 3618 (1977).
[24] We have reset the $\mathbf{G}=0$ component of both V_{ion} and V_H to zero in Fig. 4, which corresponds to a uniform energy shift.
[25] The charge flow in bulk graphite was investigated in analogy to the procedure used for nanotubes, by subtracting the superposed charge densities of graphene monolayers from the total charge density of graphite. In hexagonal graphite with AB stacking, we observed only a minute charge transfer between the two inequivalent atoms. The direction of the charge transfer, involving the π electron system, was towards the atom facing neighboring atoms in the adjacent layers.
[26] J.M. Schön, Ch. Kloc, and B. Batlogg, Nature (London) **406**, 702 (2000); *ibid.*, **408**, 549 (2000).
[27] L.A. Girifaloco and R.A. Ladd, J. Chem. Phys. **25**, 693 (1956).
[28] M.C. Schabel and J.L. Martins, Phys. Rev. B **46**, 7185 (1992).